TiO$_2$/Clay Minerals (Palygorskite/Halloysite) Nanocomposite Coatings for Water Disinfection

Dionisios Panagiotaras, Dimitrios Papoulis, Elias Stathatos

Abstract—Microfibrous palygorskite and tubular halloysite clay mineral combined with nanocrystalline TiO$_2$ are incorporating in the preparation of nanocomposite films on glass substrates via sol-gel route at 450°C. The synthesis is employing nonionic surfactant molecule as pore directing agent along with acetic acid-based sol-gel route without addition of water molecules. Drying and thermal treatment of composite films ensure elimination of organic material lead to the formation of TiO$_2$ nanoparticles homogeneously distributed on the palygorskite or halloysite surfaces. Nanocomposite films without cracks of active anatase crystal phase on palygorskite and halloysite surfaces are characterized by microscopy techniques, UV-Vis spectroscopy, and porosimetry methods in order to examine their structural properties.

The composite palygorskite-TiO$_2$ and halloysite-TiO$_2$ films with variable quantities of palygorskite and halloysite were tested as photocatalysts in the photo-oxidation of Basic Blue 41 azo dye in water. These nanocomposite films proved to be most promising photocatalysts and highly effective to dye's decoloration in spite of small amount of palygorskite-TiO$_2$ or halloysite-TiO$_2$ catalyst immobilized onto glass substrates mainly due to the high surface area and uniform distribution of TiO$_2$ on clay minerals avoiding aggregation.

Keywords—Halloysite, Palygorskite, Photocatalysis, Titanium Dioxide.

I. INTRODUCTION

DUE to the continuously growth of the earth's population and enhance of the human society needs, the environmental risk became one of the most important threats. Water pollution has been increased through time, while a variety of organic and inorganic substances degrade the water quality. In the case of organic pollutants, azo dyes are being used in huge quantities for example in the textile industry. The presence of dye in the wastewater of the textile industry affects the photosynthetic process and generates toxicity to the aquatic organisms and also humans [1]-[3]. In addition they are very stable to ultraviolet and solar light irradiation and they cannot be treated by using conventional methods [4]-[7]. For these reasons Advanced Oxidation Processes or Technologies (A.O.P. or A.O.T.) have been used in order to decompose this effluent. Photocatalysis as an A.O.T. method can be successfully applied to the oxidation and final removal of azo dyes. However, degradation of various organic pollutants by photocatalysis, using wide band gap semiconductors under UV or solar light, has been extensively studied [8]-[10]. Among them, TiO$_2$ is a relatively inexpensive semiconductor which exhibits high photocatalytic activity, non-toxicity and stability in aqueous solutions, [11], [12]. Furthermore, the synthesis of mesoporous nanocrystalline anatase TiO$_2$ particles, films or membranes has extended their use in environmental remediation [13]. One serious problem using TiO$_2$ powders as a photocatalyst is its agglomeration to large particles. Moreover, TiO$_2$ powders cannot easily be recovered from aquatic systems when they are used for water treatment. Therefore, much research has been carried out to immobilize TiO$_2$ catalyst onto various substrates as thin films and membranes in order to enhanced the photocatalytic activity and extend their field of applications [14]-[16].

Another approach to enhance the photocatalytic properties of the catalysts is the promotion of their porous structures. Among others, glass slides and fibers, membranes, activated carbon and zeolites are used as supports for TiO$_2$ particles [17]-[19]. The efficiency of photocatalytic procedure is generally decreases with catalyst immobilization as the illuminated total surface area is lower than the case of pure TiO$_2$ powder.

However, the use of highly porous materials such as clay minerals can be considered as alternative substrates for TiO$_2$ immobilized particles [20], [21]. Halloysite clay mineral with tubular structure could be considered as suitable and also cheap material for TiO$_2$ particles immobilization [22], [23]. In addition palygorskite clay mineral microfibers combined with TiO$_2$ have been used for the decomposition of NO$_x$ gases and toluene [24], [25].

In this work we present the fabrication of thin mesoporous nanocrystalline TiO$_2$ composite films with halloysite and palygorskite clay minerals. The formation of the mesoporosity of the films ought to a template technique based on the sol-gel method with surfactant molecules. The enhanced photocatalytic activity of TiO$_2$ nanoparticles in combination with halloysite nano tubes and palygorskite microfibers was examined to the discoloration of azo-dye Basic Blue 41 in aqueous solutions. The synergistic effect between TiO$_2$ and clay minerals was also tested in spite of small amount of TiO$_2$ catalyst immobilized onto the glass substrate.

II. MATERIALS AND METHODOLOGY

A. Chemical Reagents

Commercially available Triton X-100 (X100, polyethylene glycol tert-octylphenyl ether), titanium tetraisopropoxide

Dionisios Panagiotaras is with the Mechanical Engineering Department, Technological-Educational Institute of Western Greece, 26334 Patras, Greece.

Dimitrios Papoulis is with the Geology Department, University of Patras, 26504 Patras, Greece.

Elias Stathatos is with the Electrical Engineering Department, Technological-Educational Institute of Western Greece, 26334 Patras, Greece (corresponding author to provide phone: 0030-2610-369242; e-mail: estathatos@teipat.gr).

(TTIP), acetic acid (AcOH), Basic Blue 41 (BB-41), silver nitrate (>99%) and all solvents were purchased from Sigma-Aldrich. Double distilled water with resistivity 18.2 MΩ (Millipore) was used in all experiments.

Palygorskite-rich samples (PAL) from Ventzia continental basin, Western Macedonia Greece. Pure and well crystalline halloysite samples (HAL) with tubular morphology were originated from Utah, USA. Both palygorskite and halloysite samples were size fractionated by gravity sedimentation to obtain sizes less than 2μm. Separation of the clay fraction was carried out by using centrifugation methods. The clay fractions of the most halloysite and palygorskite-rich samples were used for the preparation of TiO_2-halloysite and TiO_2-palygorskite nanocomposites.

B. Sol-Gel Synthesis

The X100 as a long chain nonionic surfactant molecule was selected as a pore directing agent in sol. Compared to other commonly used toxic and ionic templating agents, X100 is relatively inexpensive, biodegradable, and easily removable. Such amphiphilic molecules exhibit the existence of ordered mesophase and the ability to adjust large inorganic clusters in aqueous condition [26], [27]. A suitable amount of X100 was homogeneously dissolved in ethanol (EtOH). Before adding alkoxide precursor, AcOH was added into the solution for the esterification reaction with EtOH. Then, titania precursor, TTIP was added at a time under vigorous stirring. The molar ratio of the materials was optimized at X100:EtOH:AcOH:TTIP = 1:69:6:1 in accordance to previous results [26]. Palygorskite powder was mixed with previous solution in various quantities following PAL weight ratio 0%, 33%, 50%, 65%, 75% compared to TiO_2. After several minutes, the dispersion was ready to be used on glass slides. Films prepared on glass slides for the five PAL-TiO_2 weight ratios will be referred as PAL0, PAL33, PAL50, PAL65 and PAL75 respectively.

In addition, halloysite (HAL) powder was mixed with previous solution in various quantities following HAL 5%, 20%, 25% and 30% weight ratio compared to TiO_2. Samples, abbreviated as HAL5, HAL20, HAL25 and HAL30, while HAL0 is referred to pure TiO_2 films. After several minutes, the dispersion was ready to be used on glass slides. Films prepared on glass slides for the four HAL weight ratios will be referred as HAL5, HAL20, HAL25 and HAL30 respectively while HAL0 represents pure TiO_2 films without the presence of halloysite.

C. Formation of TiO_2 Thin Films and Powders

Borosilicate glass with a size of L75mm (effective L60) × W25mm × T1mm was used as a substrate for fabricating immobilized PAL-TiO_2 and HAL-TiO_2 thin films. Before coating, the substrate was thoroughly cleaned with detergent and washed with water and acetone. The glasses were finally dried in a stream of nitrogen. A home-made dip-coating apparatus equipped with a speed controller to maintain a withdrawal rate of ~10cm/min was used to dip in and pull out the substrate from the sol. After coating, the films were dried

at room temperature for 1hr, calcined in a multi-segment programmable furnace (PLF 110/30, Protherm) at a ramp rate of 5ºC/min to 450ºC for 15 min, and cooled down naturally. Only one layer of catalyst was formed for all PAL-TiO_2 and HAL-TiO_2 ratios. In the case that powders of the above mentioned samples were prepared, the solutions were put in a rotary evaporator in order to remove the solvent. Then the viscous sols were heat-treated for 2 hours at 450ºC instead of 15min as in making thin films in order to remove all the organic content. In this case the heating ramp rate was 1ºC/min.

D. Instrumentation for Materials Characterization

A Bruker D8 Advance diffractometer with CuKα (λ = 1.5406Å) radiation and Bragg-Brentano geometry was employed for X-ray diffraction (XRD) studies of the PAL-TiO_2 and HAL-TiO_2 catalyst. Nitrogen intrusion/extrusion curves were measured with a Micromeritics Tristar 3000 and the surface area, porosity, and pore size distribution were derived by differentiating them according to BET method for the HAL-TiO_2. However, Hg porosimetry measurements were performed for PAL-TiO_2, instead of BET measurements that are, usually, used for the characterization of titania films. Hg porosimetry measurements are performed in order to obtain information for pore sizes larger than 0.5μm, which are not attainable by gas sorption.

For porosity measurements, the mercury intrusion curves of all samples were taken with a Quantachrome PoreMaster 60 Mercury Porosimeter while the surface area, porosity, and pore size distribution were derived by curves' differentiation. For the visual morphology of PAL-TiO_2 and HAL-TiO_2 nanostructure, an environmental scanning electron microscope (FESEM, Zeiss SUPRA 35VP) was used and inspect film homogeneity. Absorption measurements of BB-41 sols were carried out with a Hitachi U-2900 UV-Vis spectrophotometer.

E. Photocatalytic Properties of Composite Films

The cylindrical reactor was used in all experiments is described elsewhere [28]. Air was pumped through the gas inlet using a small pump to ensure continuous oxygen supply to the solution while simultaneously the air agitates it. Four black light fluorescent tubes with nominal power 4 W were placed around the reactor. The whole construction was covered with a cylindrical aluminum reflector. Cooling was achieved by air flow from below the reactor using a ventilator. In the case of PAL-TiO_2 films, the catalyst was in the form of four borosilicate glasses, covered on one side with nanocrystalline PAL-TiO_2 film in various w/w proportions specified as samples PAL0-PAL4. The total surface area of the films was approximately 60cm^2 while the photocatalyst mass was 12mg. In the case of HAL-TiO_2 films, the catalyst was also in the form of four borosilicate glasses, covered on one side with nanocrystalline HAL%-TiO_2 films.

The total surface of the photocatalyst films was also approximately 60cm^2 while the catalyst mass was approximately 50mg. The intensity of radiation reaching the surface of the films on the side facing lamps was measured with a Solar Light PMA-2100 UV-Photometer and found

equal to 0.9mW/cm^2. The reactor was filled with 80 ml of 2.5x10^{-5}M BB-41 aqueous solution. This dye is strongly adsorbed on TiO$_2$ modified films. For this reason, we stored the solution in the dark in the presence of the photocatalyst for an hour and all photocatalytic results were obtained after equilibrium.

The photo-discoloration process of the dye was examined by monitoring the absorption maximum of the BB-41 solution (at 610nm) in various irradiation times. Photo-discoloration rate of BB-41 was calculated by the formula:

$$r = \frac{C_0 - C}{C_0} \qquad (1)$$

where C$_0$ is the initial concentration of BB-41 solution and C is the final concentration after irradiation with UV light. Discoloration efficiency is determined as:

$$efficiency\% = \frac{C_0 - C}{C_0} 100\% \qquad (2)$$

For the repeated use of the photocatalysts, the films were washed with double distilled water and dried at 80^{0}C while no further treatment was followed for the films. Adsorption of BB-41 on PAL-TiO$_2$ and HAL-TiO$_2$ films was examined under dark and after 1 hour presence of the films in dye's aqueous solution.

III. RESULTS AND DISCUSSION

A. HAL-Tio$_2$ and PAL-Tio$_2$ Nanocomposite Films Structural Characteristics

The composite HAL-TiO$_2$ and PAL-TiO$_2$ films prepared on borosilicate glass substrates for different weight proportions as described in experimental section, subjected to calcination at relatively high temperature (450^{0}C) for removing the organic template. The crystallinity of the films was examined in order to detect any differences to the crystal structure of halloysite and palygorskite after heating and the crystal phase of resulting nanocomposite TiO$_2$. The XRD patterns of all films are presented in Figs. 1 (a) and (b). Strong reflection at 2θ=12.2^0 is corresponded to halloysite 7Å, while a less intensive reflection at 2θ equal to 8.80^0 corresponds to halloysite 10Å (Fig. 1 (a)).
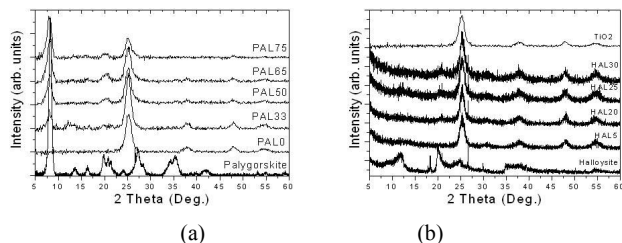

(a)   (b)

Fig. 1 XRD patterns of (a) PAL-TiO$_2$ and (b) HAL-TiO$_2$ nanocrystalline films

The main peak of halloysite 7Å seems that is remaining after heating but it is much lower mainly to the low amount of the mineral in films proving the remaining crystallinity of the clay mineral. A second reason is probably the partial dehydration of halloysite due to the temperature applied for the synthesis of the films. It should be noted that in this sample (Fig. 1 (a)) low amounts of quartz are also present (main reflections observed at 26.60^0 and 20.80^0).

Titania pure nanocrystalline film (HAL0) is also presented in Fig. 1 (b), where a reflection (101) of anatase form at 2θ=25.1^0 is observed. The two basic reflections at 2θ=12.2^0 and 2θ=25.1^0 for HAL and TiO$_2$ are maintained at the rest of samples with different intensity ratio because of the variable proportion between them. The grain size for TiO$_2$ has been calculated from XRD patterns using Scherrer's equation: D=0.9λ/(s cosθ), where λ is the wavelength of the X-ray and s is the full width (radians) at half maximum (FWHM) of the signal.

TABLE I
STRUCTURAL CHARACTERISTICS OF HAL-TiO$_2$ AND PAL-TiO$_2$ FILMS

Sample	Total pore volume Vp (cm^3/g)	Specific surface area S (m^2/g)	Total porosity φ(%)	Mean pore diameter D$_{por}$ (nm)
Halloysite	0.125	50.9	24.46	9.85
TiO$_2$	0.133	121.3	33.58	4.78
HAL5	0.165	108.6	39.10	6.09
HAL20	0.155	77.5	37.62	7.98
HAL25	0.171	95.3	39.95	7.20
HAL30	0.159	106.2	38.21	6.01
Palygorskite	3.14	123.1	85.80	18.0
PAL33	0.77	65.9	63.50	30.1
PAL50	0.92	82.2	66.20	36.0
PAL65	1.00	100.0	67.50	26.5
PAL75	1.21	95.1	70.50	24.7

The crystallite size for TiO$_2$ is calculated 7.5, 8.1, 11.3, 8.5 and 9.4nm for samples HAL0, HAL5, HAL20, HAL25 and HAL30 respectively. Strong reflection at 2θ=8^0 (Fig. 1 (b)) is corresponded to palygorskite proving the enhanced crystallinity of the clay mineral. The peaks at 2θ=13.7^0, 16.3^0, 19.8^0, 20.7^0 represent the Si-O-Si crystalline layer in the clay. Titania pure nanocrystalline film (S0) is also presented in Fig. 1 (b) where a reflection (101) of anatase form at 2θ=25.1^0 is observed. The two basic reflections at 2θ=8^0 and 2θ=25.1^0 for PAL and TiO$_2$ are maintained to the rest of samples with different intensity ratio because of the variable proportion between them. The grain size TiO$_2$ has been calculated from XRD patterns using Scherrer's equation:

$$D=0.9λ/(s \cosθ)$$

where λ is the wavelength of the X-ray and s is the full width (radians) at half maximum (FWHM) of the signal. The crystallite size for TiO$_2$ is calculated 14.5, 17.1, 15, 16.7 nm for samples PAL0, PAL33, PAL50, PAL65, and PAL75 respectively. All the peaks indicated that the crystal phase of the materials containing titania was anatase and the relatively small width of peaks indicated that the size of the nanocrystallites was less than 17nm for PAL-TiO$_2$ and less

than 12nm for HAL-TiO$_2$. It should be noted that it is evident from the XRD patterns that the calcination at 450^{0}C for 15min did not cause any phase transformation or distraction of palygorskite and halloysite.

Because of the difficulty in directly characterizing the porosity of immobilized HAL-TiO$_2$ and PAL-TiO$_2$ thin films, the characterizations were carried out on the corresponding particles. The structural characteristics of HAL-TiO$_2$ and PAL-TiO$_2$ particles regarding the specific surface area S, the total pore volume V$_p$, the mean pore diameter D$_{por}$, and the total porosity φ were calculated for all samples and they are presented in Table I. Pure halloysite has relatively large pore volume and similar to that obtained for pure TiO$_2$ while their mixtures possess slightly greater values. As it concerns the particle surface areas, in the case of pureTiO$_2$ a relatively high value of 121.3 m^2/g is measured and 50.9 m^2/g for halloysite. All other samples with different proportions of halloysite in TiO$_2$ matrix appear intermediate values for particle surface areas as they appear in Table I. Moreover, high values for the specific surface area of all samples are also measured for the palygorskite samples (Table I). Between samples of PAL/TiO$_2$ composite material, PAL65 showed the highest value for particle surface area equal to100 m^2/g.
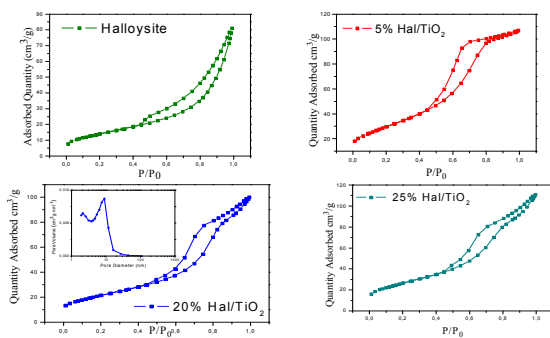

Fig. 2 Sorption-desorption isotherms and pore size distribution (20% in Halloysite) for several %wt of Halloysite in composite Halloysite-TiO$_2$ material

The nitrogen intrusion/extrusion curves of samples HAL5, HAL20 and HAL25 are presented in Fig. 2 and the pore size distribution for HAL20 as an example appear as an inset of Fig. 2.
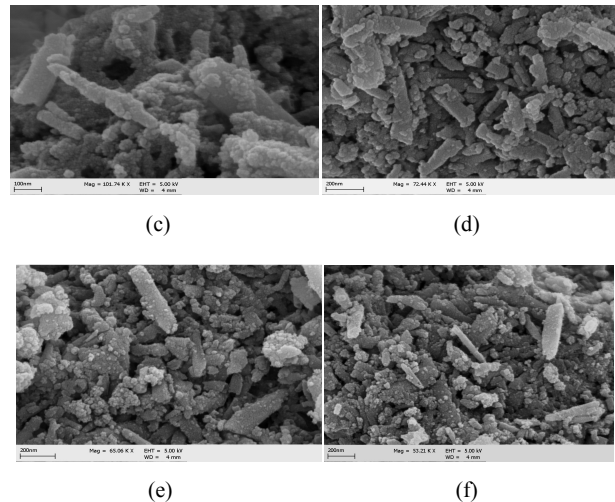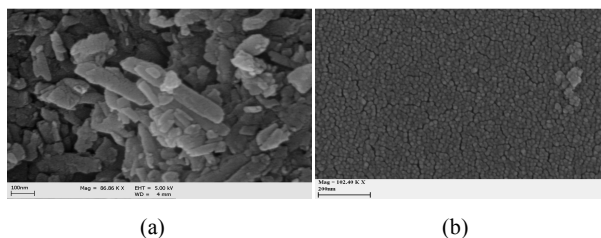

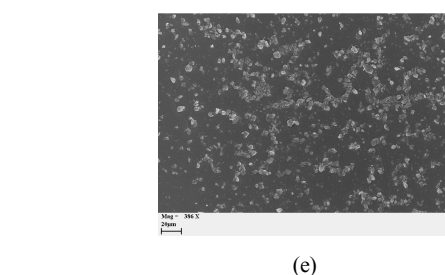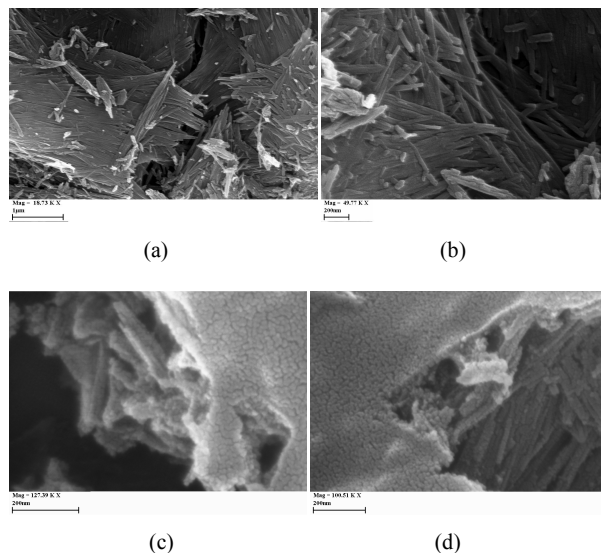Fig. 3 SEM images of: (a) Halloysite powder, (b) pure TiO$_2$, (c) HAL5, (d) HAL20, (e) HAL25 and (f) HAL30 films

Fig. 4 SEM images: of palygorskite fibers (a) in low and (b) high magnification. Modification with TiO$_2$ particles (composite PAL-TiO$_2$) film (PAL65) appear in (c) and (d) in high magnification. (e) Surface of PAL65 film

For the PAL-TiO$_2$ samples the mercury intrusion curves of all samples were also measured and the pore size distributions were derived by their differentiation and the data are presented in Table I. From data presented for all samples is obvious that

palygorskite material is highly porous (85.8%). However, a narrow distribution of palygorskite nanofibers pore size was monitored which is also maintained in the case that TiO_2 nanoparticles are used to form a composite material.

Nevertheless, TiO_2 particles are also porous (53.9%) while porosity of the composite PAL-TiO_2 material takes values among those referred for palygorskite and TiO_2 as it is also expected. This porosity is, also, apparent in SEM images shown in Fig. 3 for the HAL-TiO_2 samples and in Fig. 4 for the PAL-TiO_2 samples. Halloysite samples are consisted of tubular particles as it can be seen in Fig. 4 (a). The average diameter of the tubes, as they were observed before modification, is 40-70nm while the length is between 100-500nm

After modification, TiO_2 nanoparticles uniform in size overlay halloysite tubes. In Figs. 3 (c)-(f) halloysite nanotubes seem to be completely covered with uniform layers of TiO_2 and uniform particle distribution. The thickness of TiO_2 film without halloysite tubular particles is around 180-200nm with only one dipping layer according to cross sectional SEM image. The homogeneity of TiO_2 particles' size and film can be seen in all images of Fig. 3. According to images of Fig. 3 the TiO_2 crystal grains have a spherical shape while they have an average size ranging from 12 to 16nm.

Palygorskite samples are consisted of fibers in planar structures as it can be seen in Figs. 4 (a) and (b). The average diameter of the fibers, as they were observed before modification, is 40nm while the length is between 500 and 2000nm (Fig. 4 (b)). After modification, TiO_2 nanoparticles uniform in size overlay palygorskite fibers. Besides, titania nanoparticles help to the stabilization of the composite material on the borosilicate glass substrate after calcination by forming stable Ti-O-Si bonds [29], [30]. In Figs. 4 (c) and (d) palygorskite microfibers seem to be completely covered with uniform layers of TiO_2 with also uniform particle distribution. The thickness of TiO_2 film without palygorskite fibers is around 180-200 nm according to a cross sectional SEM image. The homogeneity of titania particles' size and film can be seen in Fig. 4 (e). The TiO_2 crystal grains have a spherical shape while they have an average size ranging from 13 to 16nm. For both HAL-TiO_2 and PAL-TiO_2 nanocomposites TiO_2 particles were also found to form aggregates on halloysite and palygorskite external surfaces but these were of uniform small size as it was also proved by porosimetry data. No cracks or peeling off traces around palygorskite and halloysite boundaries were observed. The films are permanently attached on the glass substrate with good adherence.

B. Photocatalytic Properties of HAL-TiO_2 and PAL-TiO_2 Films

Titanium dioxide mediated photo-degradation involves the generation of electron-hole pairs [11], which migrate to the photocatalyst surface forming surface bound hydroxyl and superoxide radicals according to following equations:

$$TiO_2 + h\nu \rightarrow e^-_{cb} + h^+_{vb}$$
$$O_2 + e^-_{cb} \rightarrow O_2^{-\bullet}$$

$$H_2O + h^+_{vb} \rightarrow {}^\bullet OH + H^+$$
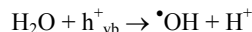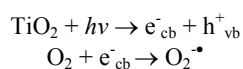
It is also well known that the hydroxyl and superoxide radicals are the primary oxidizing species in the photocatalytic process. These oxidative reactions result in the photodiscoloration of dyes as target pollutants in water. Photocatalytic experiments were undertaken on Basic Blue 41 to evaluate HAL-TiO_2 and PAL-TiO_2 composite catalyst in films as shown in Figs. 5 (a) and (b) respectively. The different weight percentages of halloysite in TiO_2 nanocrystalline films showed variations to the photocatalytic activities of the films. The rate of discolorization was monitored with respect to the change in intensity with time of the absorption peak at 610nm. The absorption peak of the dye diminished with time and disappeared during the reaction indicating that it had been decomposed. Besides, the UV illumination was started after one hour of the photocatalyst presence in dye's sol in order to be in equilibrium before illumination. The results also show that there was no direct photolysis of BB-41 in the absence of any photocatalyst. In the case of HAL20 a complete decolorization was reached within 140min of illumination implied the synergistic effect between clay mineral and TiO_2 by preparing highly porous HAL-TiO_2 catalysts (Fig. 5 (a)). However, the further addition of halloysite in films caused a slight decrease on the photocatalytic activity of films mainly at early stage of the procedure.
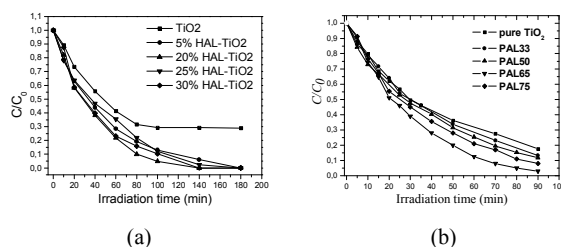

Fig. 5 (a) Photo-discoloration of BB-41 by TiO_2 films in presence of different weight percentages of halloysite under UV light. (b) Photodecoloration of BB-41 by different PAL-TiO_2 catalysts

Moreover, considering the small amount of TiO_2 catalyst immobilized onto the substrate, the HAL-TiO_2 films were highly efficient to degrade the azo dye. As a consequence, the tubular nanocomposite materials can be an alternative substrate for the growth of nanoparticle TiO_2 achieving an efficient photocatalyst. Various ratios of palygorskite-TiO_2 showed differences to the photocatalytic activities of the films (Fig. 5 (b)). The rate of discolorization was monitored with respect to the change in intensity with time of the absorption peak at 610 nm. The absorption peak of the dye diminished with time and disappeared during the reaction indicating that it had been degraded. Besides, the UV illumination was started after one hour of the photocatalyst presence in dye's sol in order to be in equilibrium before illumination. The results also showed that there was no direct photolysis of BB-41 in the absence of photocatalysts. In the case of PAL65 a complete discolorization was reached within 90 min of illumination

implied the synergistic effect between palygorskite and TiO_2 by preparing highly porous PAL-TiO_2 catalysts. However, the further addition of palygorskite in films (PAL75) caused a slight decrease on the photocatalytic activity of films. Moreover, considering the small amount of TiO_2 catalyst immobilized onto the substrate, the PAL-TiO_2 films were highly efficient to degrade the organic dye. Also from data of Fig. 5 (b) seems that palygorskite has a low photocatalytic response in UV light most probably to the presence of light activated oxides that contains such as Fe_2O_3, TiO_2 or the combination of them with MgO or CaO. As a consequence, the microfibrous nanocomposite materials can behave as photocatalysts acting separately from anatase nanoparticles, showing in this way a synergistic effect. The enhanced performance of S3 compared to the rest of the samples is attributed to the better particle surface area.
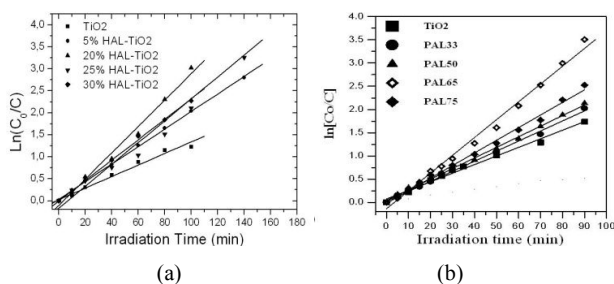

Fig. 6 Ln(C_0/C) as a function of irradiation time for: (a) HAL-TiO_2 and (b) PAL-TiO_2 photocatalysts

In both HAL-TiO_2 and PAL-TiO_2 nanocomposites decomposition kinetics of BB-41 has been observed to follow first-order kinetics and it is well established that photo-discoloration experiments follow Langmuir-Hinshelwood model, where the reaction rate, r, is proportional to the surface coverage, θ, according to the following equation, [31]:

$$r = -\frac{dC}{dt} = k_1\vartheta = \frac{k_1KC}{1+KC} \quad (3)$$

where k_1 is the reaction rate constant, K is the adsorption coefficient of the reactant and C is the reactant concentration. In the case that C is very small, KC factor is negligible in respect to unity and the above equation describes first-order kinetics. The integration of the above equation yields to the following equation:

$$-\ln\left(\frac{C}{C_0}\right) = k_{app}\,t \quad (4)$$

with limit condition that on t=0 we have the initial concentration C_0. k_{app} is the apparent first-order rate constant. Discoloration kinetics of BB-41 in presence of different HAL proportions in TiO_2 nanocrystalline films is presented in Fig. 6 (a). The maximum value for rate constant was calculated for sample HAL20 ($29.8\times10^{-3}min^{-1}$) while the value for pure TiO_2 film was estimated at $12.9\times10^{-3}min^{-1}$ (Table II). Furthermore,

all the samples HAL-TiO_2 exhibited better performance than pure TiO_2. We mainly attribute this behavior to the internal light scattering because of the presence of the halloysite.

In addition discoloration kinetics of BB-41 in presence of different PAL/TiO_2 proportions is presented in Fig. 6 (b). The maximum value for rate constant was calculated for sample PAL65 ($38\times10^{-3}min^{-1}$) while the value for pure TiO_2 film was estimated at $18\times10^{-3}min^{-1}$ (Table II). Furthermore, all the samples PAL/TiO_2 exhibited better performance than pure TiO_2. This is attributed to better structural characteristics of the films compared to pure titania film tabulated at porosity and particle surface area. Besides from data of Table II is obvious that the adsorbed quantity of BB-41 is higher in the case that palygorskite/TiO_2 composite material is used.

The above findings for the HAL-TiO_2 and PAL-TiO_2 nanocomposites could be also attributed to better structural characteristics of the films compared to pure TiO_2 film mainly tabulated at porosity and total pore volume. However, the rate of dye discolorization depends on adsorption of the dye into the catalyst porous structure. Finally, it has been found that the same photocatalysts can be used in several photocatalytic cycles without remarkable loss to their efficiency.

IV. CONCLUSIONS

Highly porous nanostructured Halloysite-TiO_2 (HAL-TiO_2) and Palygorskite-TiO_2 (PAL-TiO_2) particles and films were synthesized via sol-gel method composed of ethanol, acetic acid, titanium tetraisopropoxide, palygorskite nanofibers and nonionic surfactant molecules as templates. Slow hydrolysis reaction and stable incorporation of inorganic network onto surfactant molecules made it possible to control the subsequent porous nanostructure.

TABLE II
CONSTANT OF BB-41 DEGRADATION RATE IN THE PRESENCE OF HALLOYSITE-TiO_2 COMPOSITE FILMS MODIFIED WITH SILVER PARTICLES

Sample	k_{app}
TiO_2	12.9
HAL5	19.8
HAL20	29.8
HAL25	24.8
HAL30	23.2
Palygorskite	6
PAL33	22
PAL50	23
PAL65	38
PAL75	27

Both the HAL-TiO_2 and PAL-TiO_2 films exhibited enhanced structural properties including crystallinity and active anatase phase, while enhanced photocatalytic properties to the discoloration of BB-41 in water were succeeded. The experiments on photocatalytic discoloration of BB-41 indicated the importance of preparing highly porous HAL-TiO_2 and PAL-TiO_2 films where a synergistic effect between halloysite tubes and palygorskite microfibers with the TiO_2 nanoparticles could be occurred.

REFERENCES

[1] G. A. Umbuzeiro, H.S. Freeman, S. H. Warren, D. P. Oliveira, Y. Terao, T. Watanabe and D. D. Claxton, "The contribution of azo dyes to the mutagenic activity of the Cristais River," *Chemosp.*, vol. 60, pp. 55-64, June 2005.

[2] Y.E. Benkli, M.F. Can, M. Turan and M.S. Çelik, "Modification of organo-zeolite surface for the removal of reactive azo dyes in fixed-bed reactors," *Water Res.*, vol. 39, pp. 487-493, January–February 2005.

[3] E. Forgacs, T. Cserháti and G. Oros, "Removal of synthetic dyes from wastewaters: a review," *Environ. Int.*, vol. 30, pp. 953-971, September 2004.

[4] V. K. Gupta, J. Rajeev, N. Arunima, A. Shilpi and M. Shrivastava, "Removal of the hazardous dye—Tartrazine by photodegradation on titanium dioxide surface," *Mat. Sci. Engineer. C*, vol. 31, pp. 1062-1067, 2011.

[5] S. L. Orozco, E. R. Bandala, C. A. Arancibia, B. Serrano, R. Suárez-Parra and I. Hernández-Perez, "Effect of iron salt on the color removal of water containing the azo-dye reactive blue 69 using photo-assisted Fe(II)/H_2O_2 and Fe(III)/H_2O systems," *J. Photochem. Photobiol. A: Chem.* Vol. 198, pp. 144–149, August 2008.

[6] T. Robinson, G. McMullan, R. Marchant and P. Nigam, "Remediation of dyes in textile effluent: a critical review on current treatment technologies with a proposed alternative," *Bioresour. Techn.*, vol. 77, pp. 247-255, May 2001.

[7] C. I. Pearce, J. R. Lloyd and J. T. Guthrie, "The removal of colour from textile wastewater using whole bacterial cells: a review," *Dyes and Pigm.*, vol. 58, pp. 179-196, September 2003.

[8] M. N. Chong, B. Jin, C.W.K. Chow and C. Saint, "Recent developments in photocatalytic water treatment technology: A review," *Water Res.*, vol. 44, pp. 2997-3027, May 2010.

[9] H. Choi, S. Al-Abed, D.D. Dionysiou, E.Stathatos and P.Lianos, "TiO_2-Based Advanced Oxidation Nanotechnologies for water Purification and Reuse," in *Sustainability Science and engineering: Sustainable Water Recycling Versus Desalination Contribution,* Sustainability Science and Engineering, vol. 2, Elsevier, 2010, pp 229-254.

[10] S. Ahmed, M. G. Rasul, W. N. Martens, R. Brown and M. A. Hashib, "Heterogeneous photocatalytic degradation of phenols in wastewater: A review on current status and developments," *Desalin.*, vol. 261, pp. 3-18, October 2010.

[11] M. I. Litter, "Heterogeneous photocatalysis: Transition metal ions in photocatalytic systems," *Appl. Catal. B: Environ.*, vol. 23, pp. 89-114, November 1999.

[12] X. M. Song, J. M. Wu, and M. Yan, "Photocatalytic degradation of selected dyes by titania thin films with various nanostructures," *Thin Sol. Film.*, vol. 517, pp. 4341-4347, June 2009.

[13] H. Choi, E. Stathatos and D. D. Dionysiou, "Photocatalytic TiO_2 films and membranes for the development of efficient wastewater treatment and reuse systems," *Desalin., vol.* 202, pp. 199-206, January 2007.

[14] M. Bizarro, M.A. Tapia-Rodríguez, M.L. Ojeda, J.C. Alonso and A. Ortiz, "Photocatalytic activity enhancement of TiO_2 films by micro and nano-structured surface modification," *Appl. Surf. Scien., vol.* 255, pp. 6274-6278, April 2009.

[15] V. A. Sakkas, Md. A. Islam, C. Stalikas and T. A. Albanis, "Photocatalytic degradation using design of experiments: A review and example of the Congo red degradation," *J. Haz. Mat.*, vol. 175, 33-44, March 2010.

[16] F. Li, S. Sun, Y. Jiang, M. Xia, M. Sun and B. Xue, "Photodegradation of an azo dye using immobilized nanoparticles of TiO_2 supported by natural porous mineral," *J. Haz. Mat.*, vol. 152, pp. 1037-1044, April 2008.

[17] X. Wang, Y. Liu, Z. Hu, Y. Chen, W. Liu, and G. Zhao, "Degradation of methyl orange by composite photocatalysts nano-TiO_2 immobilized on activated carbons of different porosities," *J. Haz. Mat.,* vol. 169, pp. 1061–1067, September 2009.

[18] G. Rose, M. Echavia, F. Matzusawa and N. Negishi, "Photocatalytic degradation of organophosphate and phosphonoglycine pesticides using TiO_2 immobilized on silica gel," *Chemosp.*, vol. 76, pp. 595-600, July 2009.

[19] C.-C. Wang, C-K Lee, M-D Lyu and L-C Juang, "Photocatalytic degradation of C.I. Basic Violet 10 using TiO_2 catalysts supported by Y zeolite: An investigation of the effects of operational parameters," *Dyes and Pigm., vol.* 76, pp. 817-824, 2008.

[20] L. Bouna, B. Rhouta, M. Amjoud, F. Maury, M.-C. Lafont, A. Jada, F. Senocq and L. Daoudi, "Synthesis, characterization and photocatalytic activity of TiO_2 supported natural palygorskite microfibers," *Appl. Clay Sci.*, vol. 52, pp. 301-311, May 2011.

[21] T. An, J. Chen, G. Li, X. Ding, G. Sheng, J. Fu, B. Mai and K. E. O'Shea, "Characterization and the photocatalytic activity of TiO_2 immobilized hydrophobic montmorillonite photocatalysts: Degradation of decabromodiphenyl ether (BDE 209)," *Catal. Today*, vol. 139, pp. 69-76, December 2008.

[22] D. Papoulis, S. Komarneni, A. Nikolopoulou, P. Tsolis-Katagas, D. Panagiotaras, H.G. Kacandes, P. Zhang, S. Yin, T. Sato and H. Katsuki, "Palygorskite- and Halloysite-TiO_2 nanocomposites: Synthesis and photocatalytic activity," *Appl. Clay Sci.,* vol. 50, pp. 118-124, September 2010.

[23] D. Papoulis, S. Komarneni, D. Panagiotaras, E. Stathatos, K. C. Christoforidis, M. Fernández-García, H. Li, Y. Shu, T. Sato and H. Katsuki, "Three-phase nanocomposites of two nanoclays and TiO_2: Synthesis, characterization and photacatalytic activities," *Appl. Catal. B: Environ.*, vol. 147, pp. 526-533, April 2014.

[24] D. Papoulis, S. Komarneni, D. Panagiotaras, A. Nikolopoulou, H. Li, S. Yind, Sato Tsugio and H. Katsuki, "Palygorskite–TiO_2 nanocomposites: Part 1. Synthesis and Characterization," *Appl. Clay Sci.,* vol. 83-84, pp. 191-197, October 2013.

[25] D. Papoulis, S. Komarneni, D. Panagiotaras, A. Nikolopoulou, K.C. Christoforidis[d], M. Fernández-Garcia, H. Li, Y. Shu and T. Sato, "Palygorskite–TiO_2 nanocomposites: Part 2. Photocatalytic activities in decomposing air and organic pollutants," *Appl. Clay Sci.,* vol. 83-84, pp. 198-202, October 2013.

[26] E. Stathatos, P. Lianos and C. Tsakiroglou, "Highly efficient nanocrystalline titania films made from organic/inorganic nanocomposite gels," *Micropor. and Mesopor. Mat.*, vol. 75, pp. 255-260, November 2004.

[27] H. Choi, E. Stathatos and D. D. Dionysiou, "Synthesis of nanocrystalline photocatalytic TiO_2 thin films and particles using sol–gel method modified with nonionic surfactants," *T. Sol. Films*, vol. 510, pp. 107-114, July 2006.

[28] E. Stathatos, D. Papoulis, C.A. Aggelopoulos, D. Panagiotaras and A. Nikolopoulou, "TiO_2/palygorskite composite nanocrystalline films prepared by surfactant templating route: Synergistic effect to the photocatalytic degradation of an azo-dye in water," *J. Haz. Mat.,* vol. 211–212, pp. 68-76, April 2012.

[29] E. Stathatos and P. Lianos, F. Del Monte and D. Levy and D. Tsiourvas, "Formation of TiO_2 nanoparticles in reverse micelles and their deposition as thin films on glass substrates," *Langm.,* vol. 13, pp. 4295-4300, August 1997.

[30] J.–C. Liu, "M_x-O_y-Si_z Bonding Models for Silica-Supported Ziegler-Natta Catalysts," *Appl. Organometal. Chem.*, vol. 13, pp. 295–302, April 1999.

[31] A.O. Ibhadon, G.M. Greenway, Y. Yue, P. Falaras and D. Tsoukleris, "The photocatalytic activity and kinetics of the degradation of an anionic azo-dye in a UV irradiated porous titania foam," *Appl. Catal. B: Environ.,* vol. 84, pp. 351-355, December 2008.

Dionisios Panagiotaras is holding a BSc in Chemistry from the University of Ioannina Greece (1994) and a Ph.D. in Geochemistry from the University of Patras Greece (2008). He is an Adjunct Assistant Professor in Environmental Geochemistry and Technology at the Department of Mechanical Engineering,

Technological Educational Institute (T.E.I.) of Western Greece, Patras, Greece. Dr. Dionisios Panagiotaras research has been published in peer reviewed scientific journals and international conferences. His research interest focused in the field of Low Temperature/Environmental Geochemistry. Specific research interests are clay mineralogy, soil and sediment geochemistry, water chemistry and water-rock interactions, chemical weathering, and environmental uses of nano scale geomaterials such as modified clay minerals-TiO_2 nanocomposites for the decomposition of organic and inorganic pollutants by photocatalytic degradation.

Dimitrios Papoulis is holding a Ph.D. in clay Mineralogy from the University of Patras Greece (2003). He is an Assistant Professor in Mineral recourses emphasizing in clays and clay minerals at the Geology Department of University of Patras, Greece. Dr. Dimitrios Papoulis research has been published in peer reviewed scientific journals and international conferences. His research interest focused in the field of clay mineralogy. Specific research interests are clay minerals genesis, natural recourses, sanitary landfills, clay based nanocomposites: synthesis, characterization and photocatalytic activities in decomposing organic and inorganic pollutants.

Professor Elias Stathatos was born in 1968 in Patras, Greece. He obtained his first degree in Physics from University of Patras and then his Ph.D. degree from Engineering Science Department also in University of Patras. Prof. Stathatos was a postdoctoral research fellow in University of Cincinnati, USA at the Civil&Environmental Engineering Dept. Professor Stathatos is the head of the Nanotechnology and advanced materials laboratory and he has more than 85 publications in peer review journals and four chapters in books which are recognized of more than 2400 citations (*h*-factor=26). He is an editorial board member for Journal of Advanced Oxidation Technologies. His research interests are focused in semiconductors synthesis and characterization. In particular, prof. Stathatos is interested in the conversion of solar into electrical energy using dye-sensitized solar cells employing nanosctuctured materials and also to the heterogeneous photocatalysis based on nanocomposite semiconducting oxides.